Electrical Conduction and Space Charge in Gamma-Irradiated XLPE

C. Mouchache, N. Saidi-Amroun, V. Griseri, M. Saidi, G. Teyssedre

Electrical Conduction and Space Charge in Gamma Irradiated XLPE

C. Mouchache, N. Saidi-Amroun, V. Griseri, M. Saidi and G. Teyssedre

***Abstract*— It is well known that ionizing radiation impact dielectric and mechanical properties of polymers, as a result of chain scission, crosslinking, and oxidation steps. The electrical conductivity is generally substantially increased after irradiation. We analyze such effects in XLPE after gamma-irradiation. Current measurements reveal a substantial increase in conductivity after irradiation at doses up to 200 kGy. Current-field characteristics change after irradiation and appear indicative of an ionic-type conduction. Space charge measurements confirm the mechanism with obvious heterocharge build-up after irradiation.**

***Index Terms*— space charge XLPE gamma irradiation radiation induced conductivity**

I. Introduction

CROSS-LINKED polyethylene (XLPE) has become the most widely used material for electrical insulation in HVDC cables. This material can accumulate charges under electrical stress, increasing the local electric field and possibly causing material aging or dielectric breakdown [1]. The investigation of ionizing radiation effects in XLPE makes sense owing to the presence of insulated cables in nuclear reactors for electrical power systems for example [2], with the cable insulation being the most sensitive part to radiation [3], [4]. Major known effects of radiation on the polymer structure are chain scission, crosslinking, and oxidation [5], [6], that can be competitive effects depending on dose rates and environment conditions. From the electrical standpoint, conductivity and dielectric losses increase have been reported [7], [8], though the trends depend on polymers and dose. The increase in dielectric permittivity and losses in non-polar materials as polyethylene can be attributed to the formation of polar groups. Electronic properties of the material may change, as a result of microstructural modification, increase in defects density with change in conduction and trapping states as well as introduction of ionizable groups. In this work, we investigate changes in conduction mechanisms introduced by gamma-irradiation at dose ranging from 60 to 200 kGy, with support from space charge measurements for guiding the interpretation. To investigate the evolution in trap characteristics with irradiation, conduction currents are analyzed as a function of field, temperature and dose, as well as space charge decay kinetics as a function of irradiated doses.

II. Experimental Set-up

A. Materials

The XLPE sheets used as test materials in this study were taken from peelings of high-voltage cables, issued from the European Artemis project, where several parts of HVAC cables were exposed to electrical and thermal aging [9]. A variety of electrical and structural characterizations has been achieved in order to investigate the effects of aging. The XLPE sheets used in this study were from a roll of cable peeling that was 150 µm thick and 80 mm wide.

The irradiation was done in air at room temperature with gamma rays of a ^{60}Co source at a dose rate of 22 Gy/min for a total dose up to 200 kGy. Such total dose is expected to provide detectable material evolution with keeping mechanical integrity and is in-line with the practice in the field of cables [2]. There was a little color change following the irradiation: the samples got slightly yellowish. No appreciable change in crystallinity and melting point was observed.

B. Current and Space Charge Measurements

Current measurements were carried out on virgin and irradiated XLPE, using a Keithley 617 ammeter with a dwell time of 2 seconds and a low ripple 35 kV DC supply from Fug GbmH as a voltage source. The samples have been metallized on both sides with a 30 nm-thick gold film with a diameter of 20 mm deposited by cold plasma sputtering. The procedure followed for all samples, involves applying 3 hours of polarization and 1 h of depolarization (voltage set to zero) at a constant temperature for electric fields ranging from 5 to 40 kV/mm. This approach has been performed at temperatures of 20, 40, 60 and 80 °C.

A standard pulsed electro acoustic (PEA) test cell was used to track the space charge distribution during a cycle of polarization/depolarization. The measurements were taken in air at atmospheric pressure and at a temperature of 25 °C. The

Submitted for publication to IEEE-TDEI.

The work is supported by French-Algerian Tassili research program in the frame of Partenariat Hubert Curien and DGSDT of Algeria.

C. Mouchache, N. Saidi-Amroun and M. Saidi are with the Physics Faculty, University of Sciences and Technology, Algiers, Algeria (e-mail: mouchachecherif.usthb@gmail.com; amnadster@gmail.com; saidimohamedster@gmail.com)

V. Griseri and G. Teyssèdre are with Laplace, University Toulouse III and CNRS, Toulouse, France (e-mail: virginie.griseri@laplace.univ-tlse.fr; gilbert.teyssedre@laplace.univ-tlse.fr)

Corresponding author: G. Teyssedre.

Color versions of one or more of the figures in this article are available online at http://ieeexplore.ieee.org

sample was placed between a high voltage top electrode made of semiconducting layer (carbon black doped polymer) and ground Aluminum electrode. As shown below, irradiated samples store very quickly electrical charges. For this reason, the calibration signal necessary for the PEA cell transfer function identification was recorded on a non-irradiated sample and used for all the tests. The pulse voltage amplitude was 500 V and the calibrating DC voltage was 1.5 kV.

III. Experimental Results

A. Current Measurements Results

Figure 1.a depicts charging current on a non-irradiated XLPE sample as a function of time for various applied electric fields and temperatures. At 20 °C a continuous decrease of the current is observed for each electric field. The decrease is faster during the first 1000 s and then becomes slower, marking the transition from transient-dominated current to conduction-dominated current. At 80 °C, the contribution of transient current is reduced compared to the one at 20 °C: at this temperature the current decreases during the first instant (about 100 s) and then gets quasi-stabilized except at the lowest field with a continuous decrease. It is also worth to note the increase of the current with increasing the electric field and the temperature.

In case of irradiated XLPE, Fig. 1b, the current decreases slowly during the polarization. The current reduction is by roughly one decade after 3 h. The contribution of transient regime to the current becomes weaker in the irradiated sample and the conduction becomes rapidly the dominant process. It is also noticed that the current density increases with increasing the temperature by almost three decades.

Figure 2 displays the evolution of current density J as function of electric field E in log-log plot at different temperatures (20 to 80 °C) for non-irradiated and gamma-irradiated XLPE. Data correspond to currents after 3 h charging time, and are considered as quasi-steady state. A linear fitting was done in order to identify the conduction mechanism governing the evolution of J(E). For non-irradiated XLPE, Fig. 2a, two linear regions were identified with different slopes for each of the temperatures 20, 40, 60°C. The intersection of fitted lines defines a threshold field [10], [11] between two conduction regimes. The same threshold (20 kV/mm) is found at 20, 40, and 60 °C. At 80°C no threshold could be identified in the applied field range, either because it is under 5 kV/mm or there is completely different mechanism of conduction at 80 °C. The slopes at low field are around 1.4, 1.1 and 1.4 respectively at 20, 40 and 60 °C, the mechanism in this region is supposed to be dominated by ohmic conduction. At high field the slope is evaluated to 3.6 for 20 and 40 °C, and 2.8 for 60 °C which is indicative of a conduction process governed by space charge limited current (SCLC). At 80 °C the slope is much lower, indicating a different dominating conduction mechanism.

For XLPE irradiated at 200 kGy (Fig. 2b), linear regions were identified with slopes of about 2 for temperatures of 40,

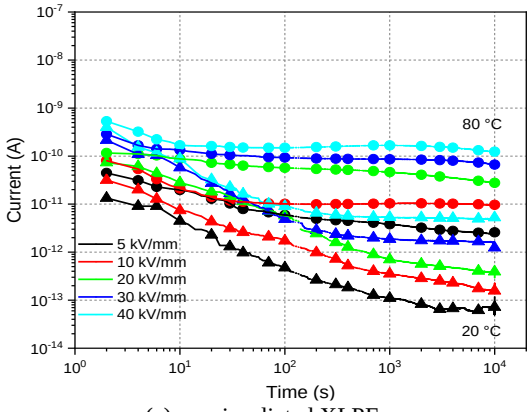

(a) non-irradiated XLPE

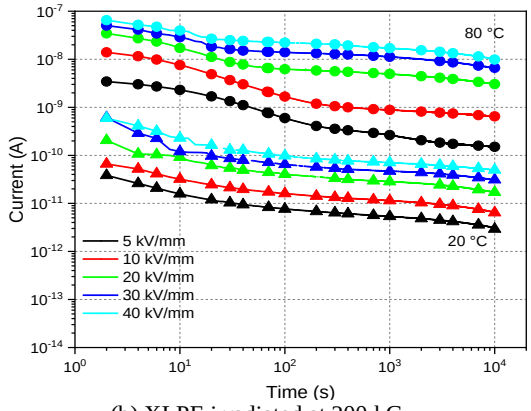

(b) XLPE irradiated at 200 kGy

Fig. 1. Charging currents measured for various electric fields at 20°C (triangles) and 80°C (circles).

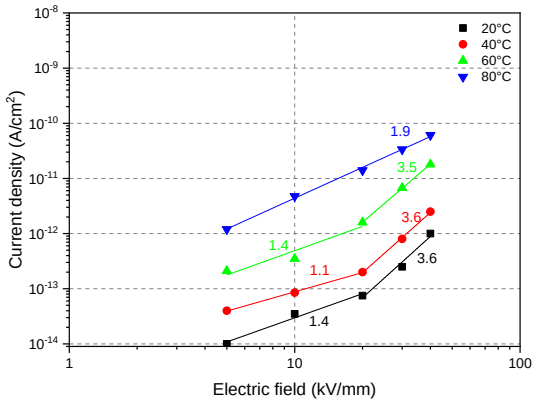

(a) non-irradiated XLPE

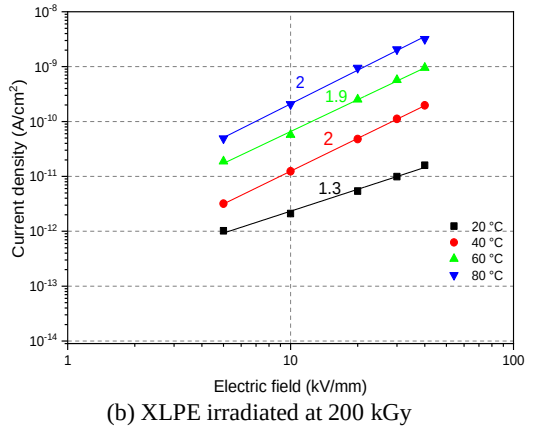

(b) XLPE irradiated at 200 kGy

Fig. 2. Current density as function of electric field in log-log scale at 20, 40, 60 and 80°C.

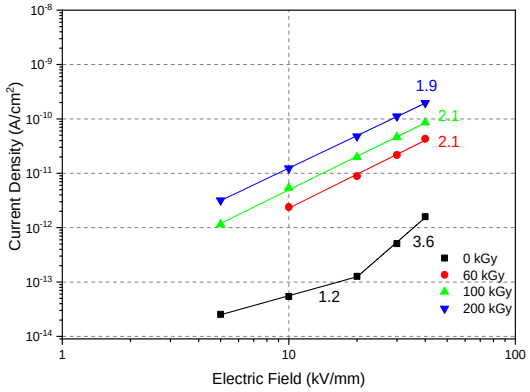

Fig. 3. Current density at 40 °C as function of electric field for non-irradiated and gamma irradiated XLPE samples.

60, and 80°C. At 20°C the slope is 1.3. The change in slope between low and high temperature indicate a change in conduction mechanism, presumably from ohmic to SCLC or ionic conduction. The conduction current increases by about 2 order of magnitudes between 20 and 80°C.

Comparing the results at 40°C for the different irradiation doses, Fig. 3, a large current increase is revealed, by a factor greater than 100 compared to non-irradiated XLPE. No threshold appears in the range of 5 to 40 kV/mm applied field for irradiated samples, and the slope is unchanged with the dose. Though the slope is typically equal to two in the SCLC conduction mechanism, depending on the physical processes at play (injection, ionic species, trapping, etc.) the interpretation of these slope values may differ.

B. Space Charge Measurements Results

Figure 4 presents the space charge distribution patterns obtained in non-irradiated XLPE during polarization under field of 40 kV/mm for 1 h. The main feature revealed in the recorded profiles is the injection of charges followed by trapping near the electrode, creating homocharge, as reported previously [12]. Negative charges are injected at the ground electrode, providing continuous charge build-up in the bulk over 1 h stressing duration. A minor quantity of positive charges was injected from the anode, with no substantial progression with time. The space charge release when the applied field is removed is depicted in Fig. 4b. The bulk of the sample has accumulated a negative charge spread throughout the insulation. The amount of negative charges progressively decreases within 1 h.

The measurement results of space charge distribution in XLPE irradiated with different doses are depicted in Fig. 5. The profiles acquired before DC stressing demonstrate that there is no residual net charge in all the samples. Upon DC stress, negative and positive charge zones are progressively produced from the first seconds of the application of external stress and the charge amount increases fast and consistently throughout this time; this behaviour is observed for the different doses. The charge clouds are next to the anode for negative charges and to the cathode for positive ones, forming hetero-charges. It is also obvious that the charged areas are well symmetrical in the form

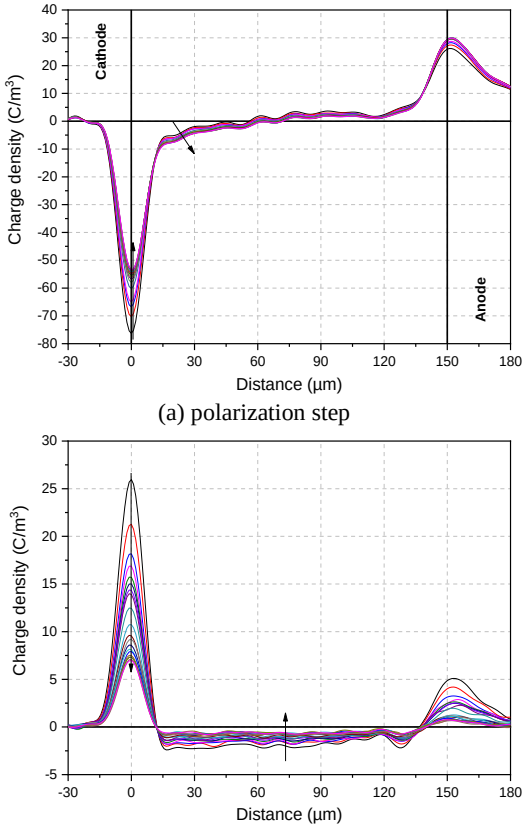

Fig. 4. Space charge profiles recorded on a non-irradiated XLPE, during 1 h of polarization/depolarization under 40 kV/mm.

of the peak with the same maximum values of charge density. Regarding the dose effect, we observe qualitatively the same behaviour for all doses.

Fig. 6 depicts the space charge patterns collected during charge relaxation (0 V applied). In the sample irradiated at 60 kGy the charges dissipate slowly during 1 h. The charges dissipation is faster as the irradiation dose increases. At 200 kGy, the maximum negative charge density is reduced by 50% in 1 h. It is also observed that the negative charge drops faster than the positive one.

IV. Discussion

A. Space charge decay and trap characteristics

To provide quantitative information of the impact of the irradiation on the space charge, a representation of the charge build-up and decay kinetics with separating the behaviour of positive and negative charges was used. The charge, measured in absolute value, was integrated using:

$$\boldsymbol{Q(t) = \int_{d_0}^{d_1} S\,|\rho(x,t)|\,dx} \qquad (1)$$

where ρ(x) is charge density, S is the electrode area and d_1 and d_0 are the limits of the heterocharge peak (positive or negative). Fig. 7 shows the evolution of negative and positive charge amount during the polarisation. For the sake of clarity, the sign of the charges is introduced in the plot. Table I gives the total charge in the sample estimated using (1) applied to the

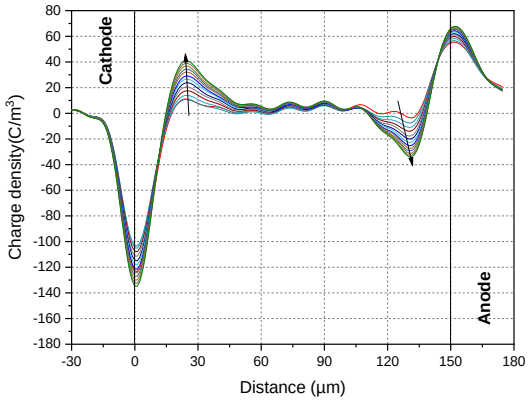

(a) 60 kGy

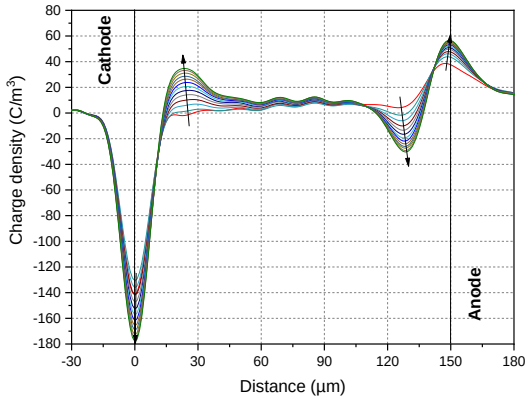

(b) 100 kGy

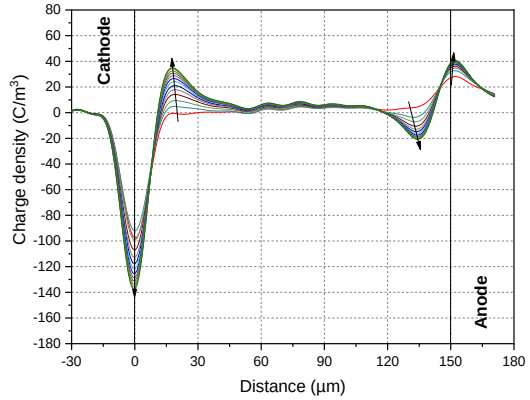

(c) 200 kGy

Fig. 5. Space charge profile recorded during 1 h under 40 kV/mm: a) 60 kGy, b) 100 kGy, c) 200 kGy.

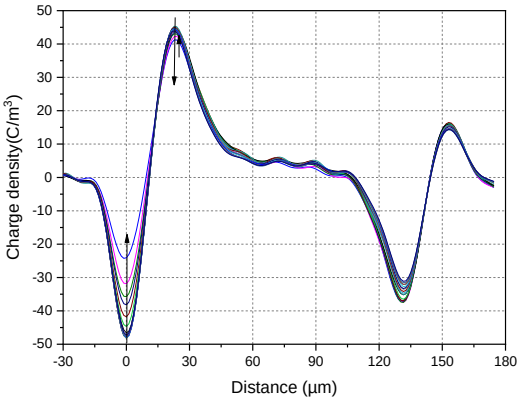

(a) 60 kGy

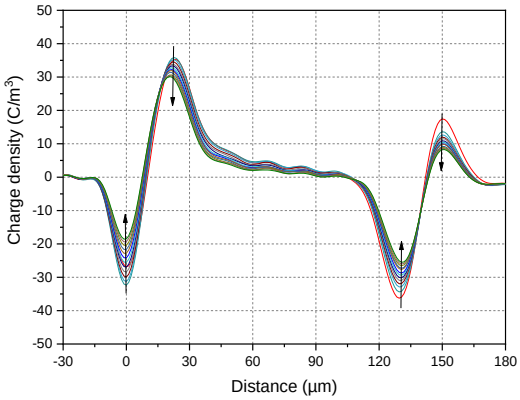

(b) 100 kGy

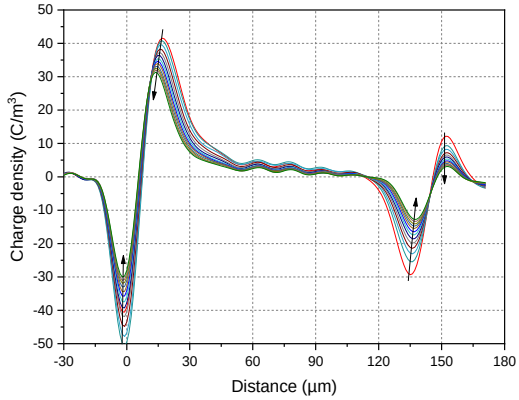

(c) 200 kGy

Fig. 6. Space charge profiles during 1 h of relaxation after polarization for 1 h: a) 60 kGy, b) 100 kGy, c) 200 kGy.

limits of the sample. The build-up of negative charges varies more with the dose compared to the positive ones. Also, the amount of hetero-charges produced decreases at high dose, consistently with report from Asch *et al* [13].

From the charge density profiles, and data of Table I, charge build-up seen in irradiated XLPE is much greater than in the non-irradiated samples. Such a huge difference between irradiated and non-irradiated XLPE is plainly connected to the influence of the energy deposited by gamma ray in the material by triggering modification of the electrical characteristics and possibly of the structure of XLPE. When the injection of charge from electrodes is the apparent mechanism responsible of space charge build-up in non-irradiated XLPE, in the irradiated XLPE the source of charges is evidently from the bulk. The positive charge produced during the DC stressing is larger than the negative one for all doses.

The charge decay during depolarization reflects trap properties in the polymer material; the discharge is expected to be slower as traps are deeper. The space charge decay is generally analyzed using an exponential decay law. To consider the contributions of de-trapping from both shallow and deep traps, the calculation based on a dual exponential function was used [14]:

$$\boldsymbol{Q(t) = Q_{01}\exp\left(-\frac{t}{\tau_1}\right) + Q_{02}\exp\left(-\frac{t}{\tau_2}\right)} \qquad (2)$$

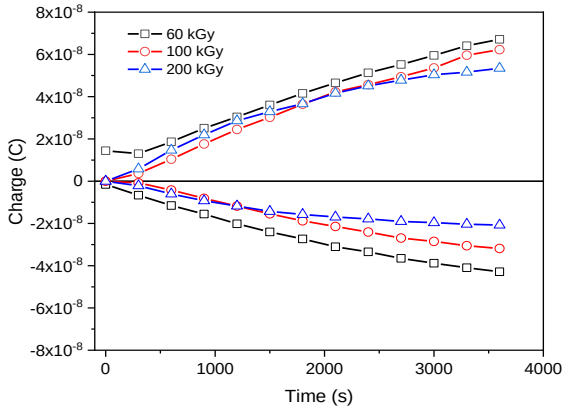

Fig. 7. Kinetic of charge build-up during polarization, with separation of positive and negative charges.

Table I

TOTAL SPACE CHARGE AMOUNT

Charging Time (min)	Charge (nC)			
	0 kGy	60 kGy	100 kGy	200 kGy
5	12	19	4.5	18
30	14	68	55	52
60	15	110	94	74

where Q_{01} and Q_{02} are the charge amounts trapped in shallow and deep traps, respectively, and τ_1 and τ_2, are the corresponding decay time constants. Fig. 8 depicts the charge decay kinetics with distinguishing the behavior of positive and negative charges. Though there is only a slightly higher amount of positive charges than of negative ones, the decay kinetics are not similar. Equation 2 was used to fit the data of Fig. 8 and the obtained fit parameters are listed in Table II. Given the strong variation in the responses, the function with decay time constant τ_1 is considered here only as an adjustment for the data at short time. The decay time constant τ_2 associated to charge escape from deep traps decreases substantially with the increase of irradiation dose and this holds for both negative and positive charges. The ratio of τ_2 between the higher and lower doses is close to 4 for both charges polarities. Values of the time τ_2 also confirm the faster discharge rate for negative charges, by a factor of about 2.

The trap energy E_t and trap density $N_t(E_t)$ have been computed based on charge decay kinetics, following two assumptions: 1) the charges do not get re-trapped once de-trapped; and 2) the recombination processes can be neglected. Equations (3) and (4) were used to compute E_t and $N_t(E_t)$, respectively, [14].

$$E_t = kT \cdot \ln(\nu \cdot t) \quad (3)$$

$$N_t^{+/-}(E_t) = \frac{t}{l^{+/-} SkTef_0(E_t)} \cdot dQ^{+/-} \Big/ dt \quad (4)$$

where k is the Boltzmann constant, T is the absolute temperature, l is the thickness of the positive (negative) charge region, ν is the attempt to escape frequency (ν=kT/h), h is Planck constant, e is the electron charge, and $f_0(E_t)$ is the initial trap occupancy (1/2). The trap distributions obtained using the exponential decaying function as inputs are plotted in Fig. 9.

The two contributions to (2) are easily distinguished for positive charge for 60 and 100 kGy doses (Fig. 9a). The maximum shallow trap density for XLPE irradiated at 60 kGy

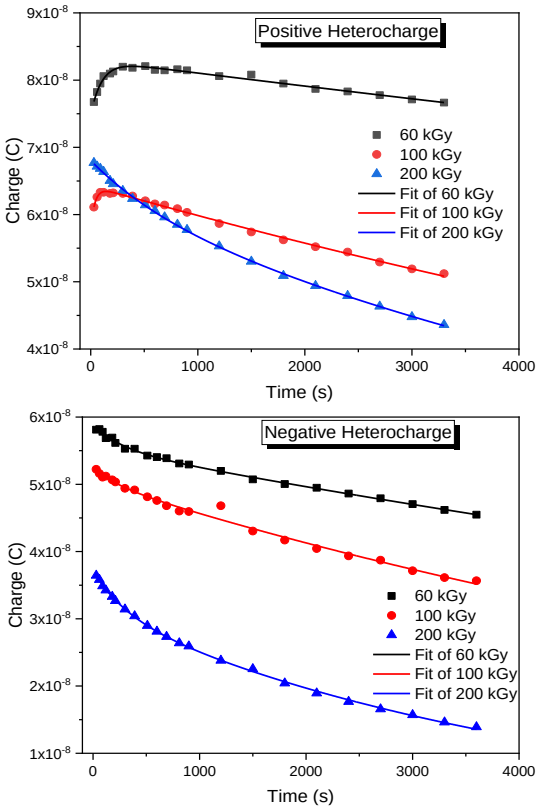

Fig. 8. Kinetic of charge decay, with separation of positive and negative charges.

is 2.2×10^{13} $m^{-3}.eV^{-1}$ at trap depth of 0.85 eV. For a sample exposed to 100 kGy of radiation, $N_t^+ = 1.8\times10^{13}$ $m^{-3}.eV^{-1}$ for E_t^+ = 0.82 eV. At 200 kGy the shallow trap peak is estimated at 0.91 eV where a shoulder barely noticeable appears as the peak due to deep traps becomes preponderant in this region. The last value of trap density was estimated just below 0.95 eV but does not reach the deep trap depth extremum. However, at this depth the trap density increases quite a lot with the radiation dose (N_t^+ = 4.4, 8.4, and 10.6 $\times10^{13}$ $m^{-3}.eV^{-1}$ for 60, 100, and 200 kGy respectively).

TABLE II

PARAMETERS DERIVED FROM FITTING CHARGE DECAY.

Parameters	60 kGy	100 kGy	200 kGy
Positive Charges			
Q_{01} (nC)	-8.2	-6.4	7.2
τ_1 (s)	104	40	726
Q_{02} (nC)	83	64	61
τ_2 (s)	41×10^3	14×10^3	9.8×10^3
R^2	0.98	0.99	0.99
Negative Charges			
Q_{01} (nC)	3	2	6
τ_1 (s)	283	234	313
Q_{02} (nC)	55	50	31
τ_2 (s)	18×10^3	10×10^3	4×10^3
R^2	0.99	0.99	0.99

For negative charges (Fig. 9b), the peak associated to the shallow traps is apparent though the amplitude is weak for all the doses. A peak maximum can be distinguished just below 0.95 eV for the dose 200 kGy.

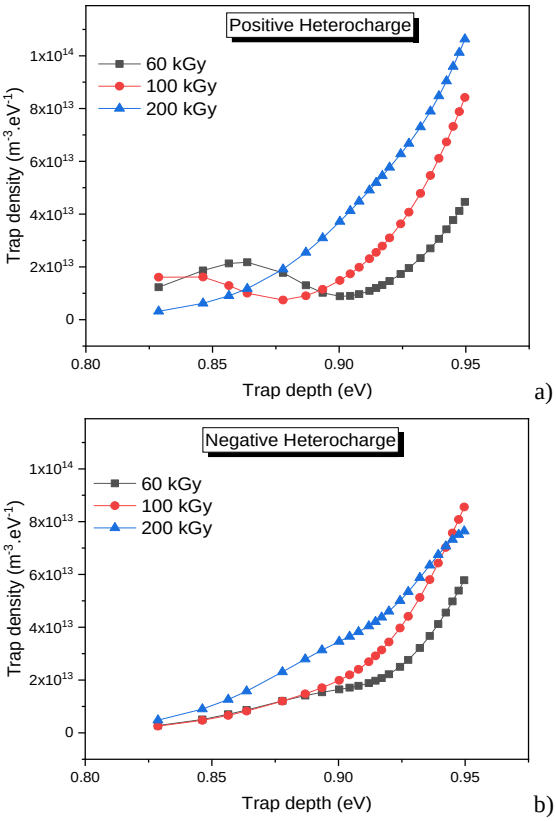

Fig. 9. Trap distributions for irradiated XLPE, a) positive charge, b) negative charge.

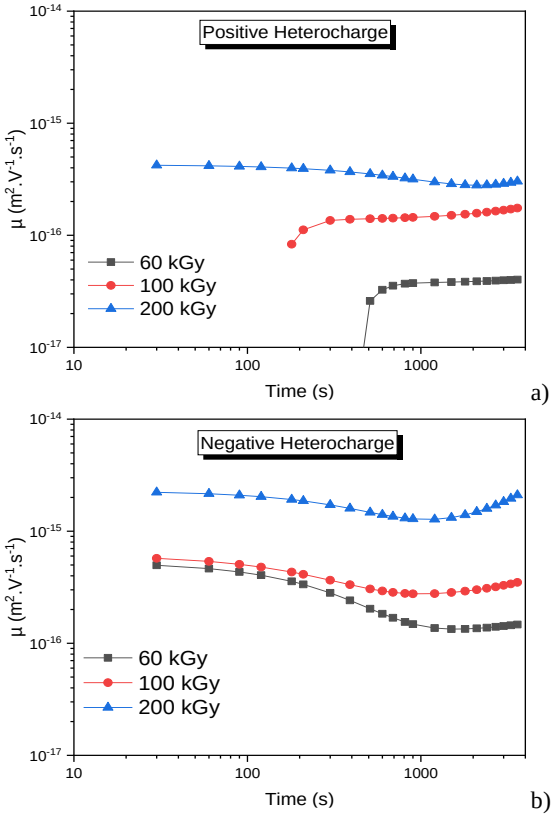

Fig. 10. Apparent mobility calculated as a function of depolarization time in irradiated XLPE at 60, 100 and 200 kGy: a) positive charge, b) negative charge.

The maximum deep trap density was not reached in 1 h relaxation time and charges in deep traps (E_t>1 eV) were not released, which is consistent with the space charge results shown in Fig. 6, indicating that charges are still present after relaxation ends.

Liu and Chen [15] and Sarathi *et al* [16] reported that when the radiation dose is increased, the trap density increases and the trapping depth decreases. The increase in deep trap density can be explained easily because gamma-irradiation changes the chemical structure of the material and is a common type of photo-oxidation process that introduces more chemical defects. The coloring of samples is an obvious sign that chemical modification of the material has occurred. A significant increase in the carbonyl absorption region (1710-1720 cm^{-1}) was observed by FTIR for all doses (results not shown here). To explain the lowering of trap depth at high dose, Suarez *et al* [17] have argued that gamma irradiation process involves crosslinking at low doses and chain scission at high doses.

Irradiation may produce electron-hole pairs or ion pairs into the material that may subsequently be pushed toward the electrodes under application of the field. The theory in terms of ions mobility would be congruent with the comparably slow charge decay and with the fact that symmetrical charge patterns are visible. The net charge decay may be explained by the movement of one polarity ions creating depletion on one side and accumulation on the other side. Radiation may also produce ionizable molecules or groups that may be subsequently dissociated under the action of the field during space charge measurements. Indeed, oxidation is known as as one of the primary modification mechanisms triggered by the irradiation [18], [19]. Fu *et al* [20] reported on much more impact on space charge accumulation when irradiation was achieved in air compared to neutral atmosphere.

B. Apparent Charge Mobility

The apparent mobility can be estimated from space charge results, and used as ageing marker to monitor changes going through the material [21]. The following relation has been used [22]:

$$\boldsymbol{\mu\,(t) = \frac{\varepsilon l^2 S^2}{Q(t)^2}\frac{dQ(t)}{dt}} \qquad (5)$$

where μ is the apparent charge mobility, ε is the material permittivity, Q (t) is the net charge at time t obtained through equation (1). To disclose the features of positive and negative charges, (5) has been applied separately for positive and negative charges [23]. The apparent mobility of the positive and negative charges as determined by (5) is shown in Fig. 10.

With increasing the irradiation dose, the apparent mobility of both positive and negative charge rises. However, the apparent mobility in positive and negative charges shows different time dependencies. According to Fig. 10a, the apparent mobility of positive charge varies from 4 10^{-17} to 3 10^{-16} $m^2.V^{-1}s^{-1}$ (at 1000 s when the dose is increased from 60 to 200 kGy. For 60 and 100 kGy the mobility, as plotted from 500 s and 150 s, respectively, until 3600 s remains rather stable. For the plotted data it is important to notice that the apparent mobility of positive charges does not change significantly over time up to 3600 s, which indicates that mainly charges from similar trap

depths are involved into the mechanism. At this stage, we can suppose that it is the deep traps that are concerned.

For negative charges, the apparent mobility ranges from 1.5 10^{-16} to 1.5 10^{-15} $m^2.V^{-1}s^{-1}$ at 1000 s when changing from 60 to 200 kGy of radiation. The mobility decreases for the first 1000 s before beginning to rise until the end of the relaxation period. Shallow traps may contribute more to the transport of negative charges in the first part than deep traps.

It is important to notice that negative charge mobility is larger than that of positive ones, suggesting that negative charges are easily detrapped as found in the previous section.

It was shown by simulation that electrons tend to be trapped into the inter-chain spaces, while hole traps are along the chain backbone. Due to the weak interaction between the trapped electrons and the nearby chemical chains, the trapped electrons are easily released. On the other hand, because intra-chain traps have higher bonding, trapped holes need more energy to be released than trapped electrons [14], [24]. This can explain the high values of mobility found for the negative charges.

C. Features of a Ionic-type Conduction

As stated in space charge measurements, the generation of hetero-charges is the main phenomenon revealed in irradiated XLPE. Based on these results, a hopping process can be a way to explain the conduction current in irradiated materials in terms of mobile ions or defect sites. It contrasts with the SCLC regime of conduction that seems to be at play in pristine XLPE considering the charge profile and J-E characteristic. A simple model first established for ionic conduction leads to a current proportional to sinh(eλE/2kT) where λ is the jump distance between potential wells [25], [26]. To account for temperature effects on the current, a thermal activation energy E_i is taken into consideration based on the Arrhenius law. When a field is applied, carriers are thought to be thermally activated above a potential well, increasing the probability that the carrier will move in the field direction. From this simplified illustration, a field-dependent mobility is obtained [27]:

$$J(E,T) = J_0 . sinh\left(\frac{e\lambda E}{2kT}\right) . exp\left(\frac{-E_i}{kT}\right) \qquad (6)$$

Fig. 11 shows the evolution of the current density as function of sinh(eλE/2kT) in XLPE irradiated at different doses. Linear variations could be obtained in all the results by fitting on the value of λ and the trend was a decrease of λ with increasing the dose. With the increase of the irradiation dose, the hopping probability between the adjacent traps centers will increase accompanying by a dramatic rise of the current. This holds for all the measurement temperatures.

Table III shows the results for the trap density as a function of irradiation dose. The trap density was estimated as $n = \lambda^{-3}$ using averaged values of λ obtained at temperatures of 40, 60 and 80°C (the deviation was typically within 0.2 nm). As expected, the trap density increases as the irradiation dose increases. The activation energy E_i decreases as the dose is increased, showing that less deep traps are created. Mouaci *et al* [28] correlated this decrease of thermal activation energy to the carbonyl groups density increase which is directly linked to oxidation rate emphasized by the irradiation in air. Carbonyl effectively form deep traps for electrons (1.6 eV or so) but more shallow for holes (0.6 eV) [29]. Many possible defects are produced by irradiation and the increase in the degree of conjugation can be a route to shallower traps. The activation

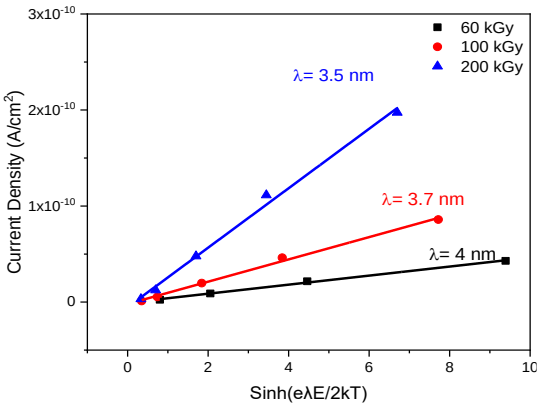

(a) 40 °C

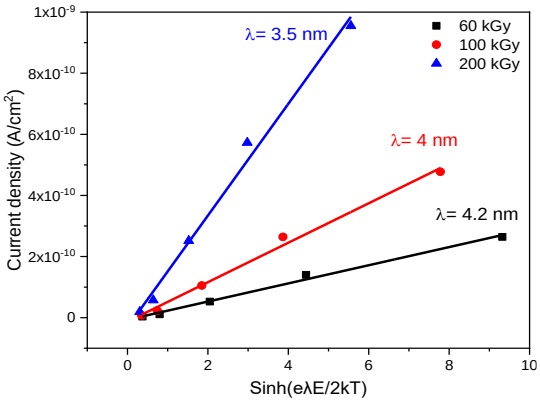

(b) 60 °C

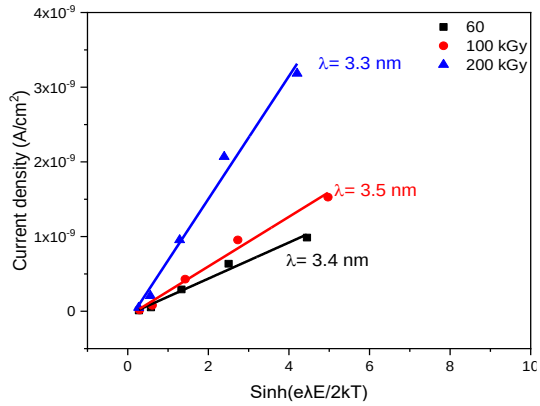

(c) 80 °C

Fig. 11. Current density versus field with a linearization of (6) for XLPE irradiated at different doses at different temperatures, a) T=40°C, b) T=60°C, c) T=80°C.

TABLE III
FITTING PARAMETERS FOR A HOPPING CONDUCTION.

Parameter	60 kGy	100 kGy	200 kGy
E_i (eV)	0.82	0.70	0.69
λ (nm)	3.9	3.7	3.4
n (m^{-3})	2.6 10^{19}	2.7 10^{19}	2.9 10^{19}

energies obtained are lower than in the analysis of space charge decay, which is explained by the fact that relatively more shallow states are involved and probed in conduction.

V. Conclusion

The space charge dynamics features revealed strong effects of irradiation in XLPE. In contrast to the un-irradiated XLPE which mainly consisted of negative charge build-up injected from the cathode and spreading in the bulk, gamma irradiated XLPE has strong hetero-charge build-up close to the two electrodes. The total amount of hetero-charge decreases with the irradiation dose after the same polarization time.

In order to analyze charge decay kinetics in gamma-irradiated XLPE, a simplified detrapping model based on shallow and deep traps was applied, revealing distinct behaviors for positive and negative charges. With increasing the irradiation dose, deep traps become preponderant, and both positive and negative trap densities rise. According to the computed values, the negative charges mobility is significantly increased with the dose. The mobility of negative charges was higher than that of positive ones. The electrical properties modifications, connected to the material's physical and chemical conditions, can be described by the obtained trapping parameters and used as ageing markers.

The current measurements revealed a dramatic increase of current in gamma irradiated XLPE compared to virgin sample. In the non-irradiated XLPE the space charge limited current is the principal mechanism dominating the conduction current, while in irradiated materials a ionic conduction process seems at play. The parameters obtained in the ionic conduction model indicate that the trap density increases with the irradiation dose and the thermal activation energy decrease. Relatively shallow traps are created with the radiation and this may explain changes in the conduction current.

References

[1] S. Le Roy and G. Teyssedre, “Ion generation and transport in low density polyethylene under electric stress,” Proc. 2015 Conf. Electr. Insul. Dielectr. Phenomena, CEIDP, pp. 63–66, 2015.

[2] S. V. Suraci, D. Fabiani, A. Xu, S. Roland, and X. Colin, “Ageing assessment of XLPE LV cables for nuclear applications through physico-chemical and electrical measurements,” IEEE Access, vol. 8, pp. 27086–27096, 2020.

[3] M. Ferry and F. Miserque, “Radio-oxidation of electric cabled models : ageing evaluation at the atomic scale,” Energies, vol. 15, n°1631, 2022.

[4] A. B. Reynolds et al., “Dose-rate effects on the radiation-induced oxidation of electric cable used in nuclear power plants,” Radiat. Phys. Chem., vol. 45, no. 1, pp. 103–110, 1995.

[5] T. Kurihara, T. Takahashi, H. Homma, and T. Okamoto, “Oxidation of cross-linked polyethylene due to radiation-thermal deterioration,” IEEE Trans. Dielectr. Electr. Insul., vol. 18, no. 3, pp. 878–887, 2011.

[6] S. Liu, L. S. Fifield, and N. Bowler, “Aging mechanisms of filled cross-linked polyethylene (XLPE) cable insulation material exposed to simultaneous thermal and gamma radiation,” Radiat. Phys. Chem., vol. 185, p. 109486, 2021.

[7] E. Suljovruji, “Dielectric studies of molecular β-relaxation in low density polyethylene: The influence of drawing and ionizing radiation,” Polymer (Guildf)., vol. 43, no. 22, pp. 5969–5978, 2002.

[8] L. Verardi, D. Fabiani, and G. C. Montanari, “Correlation of electrical and mechanical properties in accelerated aging of LV nuclear power plant cables,” 2014 Int. Conf. High Volt. Engg. ICHVE, pp. 1–4, 2014.

[9] G. Teyssedre, C. Laurent, and G. C. Montanari, “Semi-quantitative analysis of photoluminescence in thermoelectrically aged cables: II-analysis of a population of cables,” IEEE Trans. Dielectr. Electr. Insul., vol. 16, no. 4, pp. 1189–1198, 2009.

[10] G. C. Montanari and P. H. F. Morshuis, “Space charge phenomenology in polymeric insulating materials,” IEEE Trans. Dielectr. Electr. Insul., vol. 12, no. 4, pp. 754–767, 2005.

[11] T. T. N. Vu, G. Teyssedre, B. Vissouvanadin, S. Roy, and C. Laurent, “Correlating conductivity and space charge measurements in multi-dielectrics under various electrical and thermal stresses,” IEEE Trans. Dielectr. Electr. Insul., vol. 22, no. 1, pp. 117–127, 2015.

[12] C. Mouchache, V. Griseri, N. Saidi-Amroun, G. Teyssedre, S. Mouaci, and M. Saidi, “Dynamic of a space charge in gamma-irradiated cross-linked polyethylene (XLPE),” Proc. 2020 IEEE 3rd Int. Conf. Dielectr. ICD, pp. 409–412, 2020.

[13] M. G. Asch, M. C. Félix, and M. R. Ongaro, “Electrisation du polyéthylène et du polystyrène après irradiation γ,” Phys. Status Solidi, vol. 17, no. 1, pp. 49–57, 1966.

[14] L. Fan et al., “An Electron and hole trap energy distribution estimation model and its application in polypropylene nanocomposites,” IEEE Trans. Dielectr. Electr. Insul., vol. 28, no. 6, pp. 1957–1963, 2021.

[15] N. Liu and G. Chen, “Changes in charge trapping/detrapping in polymeric materials and its relation with aging,” in 2013 Annual Report Conference on Electrical Insulation and Dielectric Phenomena, 2013, pp. 800–803.

[16] N. Guvvala, B. Nageshwar Rao, and R. Sarathi, “Effect of gamma irradiation on space charge and charge trap characteristics of epoxy–MgO nanocomposites,” Micro & Nano Lett., vol. 14, pp. 1334–1339, 2019.

[17] J. C. M. Suarez, E. E. da Costa Monteiro, and E. B. Mano, “Study of the effect of gamma irradiation on polyolefins—low-density polyethylene,” Polym. Degrad. Stab., vol. 75, no. 1, pp. 143–151, 2002.

[18] D. Kostoski, J. Dojčilović, L. Novaković, and E. Suljovrujić, “Effects of charge trapping in gamma irradiated and accelerated aged low-density polyethylene,” Polym. Degrad. Stab., vol. 91, no. 9, pp. 2229–2232, 2006.

[19] G. Chen, A. E. Davies, and H. M. Banford, “Influence of radiation environments on space charge formation in γ-irradiated LDPE,” IEEE Trans. Dielectr. Electr. Insul., vol. 6, no. 6, pp. 882–886, 1999.

[20] M. Fu, G. Chen, L. A. Dissado, J. C. Fothergill, and C. Zou, “The effect of gamma irradiation on space charge behaviour and dielectric spectroscopy of low-density polyethylene,” Proc. 2007 Int. Conf. Solid Dielectr. ICSD, pp. 442–445, 2007.

[21] G. C. Montanari, D. Fabiani, M. Melloni, and F. Palmieri, “Diagnostic markers for ac power cable insulation aging based on space charge measurements,” Proc. IEEE Int. Symp. Electr. Insul., pp. 464–467, 2002.

[22] G. Mazzanti, G. C. Montanari, and J. M. Alison, “A space-charge based method for the estimation of apparent mobility and trap depth as markers for insulation degradation-theoretical basis and experimental validation,” IEEE Trans. Dielectr. Electr. Insul., vol. 10, no. 2, pp. 187–197, 2003.

[23] W. Wang, T. Takada, Y. Tanaka, and S. Li, “Trap-controlled charge decay and quantum chemical analysis of charge transfer and trapping in XLPE,” IEEE Trans. Dielectr. Electr. Insul., vol. 24, no. 5, pp. 3144–3153, 2017.

[24] Y. Wang, J. Wu, and Y. Yin, “Investigation of surface trap distribution in LDPE/SiO_2 nanocomposite based on simultaneous observation of space charge and relaxation current,” IEEE Trans. Dielectr. Electr. Insul., vol. 23, pp. 3486–3493, 2016.

[25] C. Guillermin, P. Rain, and S. W. Rowe, “Transient and steady-state currents in epoxy resin,” J. Phys. D. Appl. Phys., vol. 39, no. 3, pp. 515–524, 2006.

[26] M. Kosaki, K. Sugiyama, and M. Ieda, “Ionic jump distance and glass transition of polyvinyl chloride,” J. Appl. Phys., vol. 42, no. 9, pp. 3388–3392, 1971.

[27] G. Teyssedre and C. Laurent, “Charge transport modeling in insulating polymers: From molecular to macroscopic scale,” IEEE Trans. Dielectr. Electr. Insul., vol. 12, no. 5, pp. 857–874, 2005.

[28] S. Mouaci, G. Teyssedre, N. Belkahla, M. Saidi, V. Griseri, and N. Saidi-Amroun, “Charge trapping and conduction in γ irradiated isotactic polypropylene,” IEEE Trans. Dielectr. Electr. Insul., vol. 24, no. 6, pp. 3821–3830, 2017.

[29] M. Unge, C. Törnkvist, and T. Christen, "Space charges and deep traps in polyethylene — Ab initio simulations of chemical impurities and defects," Proc. 2013 Int. Conf. Solid Dielectr. ICSD, pp. 935-939, 2013.